Physica B 432 (2014) 105–110

Contents lists available at ScienceDirect

Physica B

journal homepage: www.elsevier.com/locate/physb

The alkali and alkaline earth metal doped ZnO nanotubes: DFT studies

Ali Ahmadi Peyghan [a], Maziar Noei [b,*]

[a] Department of Chemistry, Faculty of Science, Central Tehran Branch, Islamic Azad University, Tehran, Iran
[b] Department of Chemistry, Mahshahr Branch, Islamic Azad University, Mahshahr, Iran

ARTICLE INFO

Article history:
Received 17 May 2013
Received in revised form
11 September 2013
Accepted 26 September 2013
Available online 7 October 2013

Keywords:
Nanostructures
Electronic structure
Ab-initio calculations

ABSTRACT

Doping of several alkali and alkaline earth metals into sidewall of an armchair ZnO nanotube has been investigated by employing the density functional theory in terms of energetic, geometric, and electronic properties. It has been found that doping processes of the alkali and alkaline metals are endothermic and exothermic, respectively. Based on the results, contrary to the alkaline metal doping, the electronic properties of the tube are much more sensitive to alkali metal doping so that it is transformed from intrinsic semiconductor with HOMO–LUMO energy gap of 3.77 eV to an extrinsic semiconductor with the energy gap of ~1.11–1.95 eV. The doping of alkali and alkaline metals increases and decreases the work function of the tube, respectively, which may influence the electron emission from the tube surface.

1. Introduction

Carbon nanotubes (CNTs) have been in the spotlight of research groups in different disciplines since the first report of their fabrication in the early 1990s [1]. This has been partly due to their fascinating electronic properties, which in the past few years have been shown to change dramatically upon exposure to different chemical environments [2,3]. Building up on these findings, a wide array of experimental and theoretical studies have been conducted since then involving various adsorbates, with a number motivated by the creation of novel nanoscale tools such as CNT-based semiconducting devices [4,5]. Moreover, numerous investigations have focused on the other stable nanotubes and their applications [6–12].

Zinc oxide (ZnO) has various applications such as in optoelectronics, sensors, spintronics, pharmaceuticals, catalysts, etc. [13–17]. It also has promising applications in piezoelectric and wireless [15] devices. The optical characteristics of zinc oxide materials seem to depend on their microstructures, morphologies, and particle sizes. ZnO nanotubes (ZnONTs), with relatively wide direct band gap, are semiconductors that are slightly dependent on their chirality and diameter [18]. Therefore, the ZnONTs are especially suitable to protect a ferromagnetic nanowire inside their cavity from oxidization, and they are also good candidates for safe biology cavities due to their innocuity [19].

Systematic investigations of the structural and electronic properties of ZnONTs have been reported [20–22]. Later, the change of electronic structure and magnetism of ZnONTs induced by C and V doping, as well as defects of Zn and O vacancies on the tube walls have been also analyzed with *ab initio* calculations [23,24]. Doping ZnO nanostructures with metal ions is a strategy to modify their electronic and optical performance and improve their applications. Ni-doped ZnO nanowire has shown considerable increase in photoluminescence [25]. High-T_C ferromagnetism has been achieved by doping ZnO with Mn^{2+} [26].

ZnO is n-type metallic due to the zinc interstitials and oxygen vacancies [27,28]. In order to improve its applications, p-type doped ZnO is needed. For a good dopant, it should have appropriate solubility and ionization energy. As we know, alkali and alkaline earth metals (AM and AEM, respectively) have good electrical and thermal conductivity, however, the doping of nanotubes with these metals has been rarely discussed even in CNTs. Therefore, herein, we report a theoretical study on the doping of selected alkali (Li, Na, K, and Rb) and alkaline earth metals (Be, Mg, Ca and Sr) on the ZnONTs through density functional theory (DFT) calculations in terms of energetic, geometric, and electronic properties of the tubes.

2. Computational methods

Geometry optimizations, energy calculations, and density of states (DOS) analysis have been performed on an armchair (3, 3) ZnONT and different X-doped ZnONT complexes (X@ZnONT, X stems for all of the dopants) using unrestricted B3LYP functional with LANL2DZ basis sets as implemented in GAMESS suite of program [29]. GaussSum program [30] has been used to obtain the DOS results. The B3LYP has been demonstrated to be a reliable and commonly used functional for studying different nanostructures [31–34]. Doping energy (E_{dop}) for the X atom has been obtained

* Corresponding author. Tel.: +98 9125759236.
E-mail address: noeimaziar@gmail.com (M. Noei).

0921-4526/$ - see front matter © 2013 Elsevier B.V. All rights reserved.
http://dx.doi.org/10.1016/j.physb.2013.09.051

using the following equation:

$$E_{dop} = E(Zn) + E(X@ZnONT) - E(ZnONT) - E(X) \quad (1)$$

where E (X@ZnONT) is the total energy of the X-doped ZnONT, E (Zn) and E (X) is referred to the energy of an isolated Zn and X atoms, respectively. The E (ZnONT) is the total energy of the pristine ZnONT. Negative value of E_{dop} indicates the exothermic nature of the doping process.

3. Results and discussion

3.1. Structure optimization and geometry

Optimized structure and geometry parameters of the (3, 3) ZnONT containing 72 atoms are shown in Fig. 1. A ZnONT can be taken as a cylinder rolled up from a single sheet of ZnO layer in such a way that two equivalent sites of the hexagonal lattice coincide. As shown in Fig. 1, the optimized diameter of the ZnONT is 5.963 Å. The average Zn–O bond length in the optimized ZnONT is about 1.914 Å, which is shorter than the bond length of 1.986 Å in wurtzite ZnO crystal [35]. The average bond angles of Zn–O–Zn and O–Zn–O are about 118°, which are close to the tetrahedral sp^2 bond angle of 120° and similar to the bond angle in the ultra-thin (2,2) CNT [36]. Calculated DOS plot reveals that the pristine ZnONT is a semiconductor with the HOMO (the highest occupied molecular orbital)/LUMO (the lowest unoccupied molecular orbital) energy gap (E_g) of 3.77 eV (Fig. 1). It should be noted that, here, the E_g also denotes the gap between SOMO (singly occupied molecular orbital) and LUMO of the open shell systems. Frontier Molecular Orbital (FMO) analysis shows that the conduction level comes mainly from Zn atoms, while valence level comes mainly from O atoms. Reducing boundary effects, atoms at the open ends of the tube have been saturated with hydrogen atoms. However, the edge states are not completely passivated. This is a common problem for the finite length nanotube calculations, but it has no influence on the analysis of electronic structure in our work. This calculation error can be ignored when the results of metal doped into the ZnONT surface are compared based on the same system and calculation method.

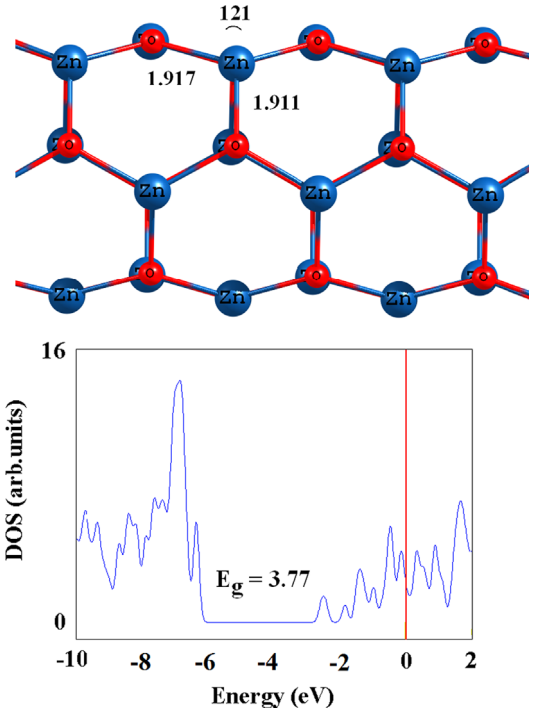

Fig. 1. Side and top view of optimized structure of armchair ZnONT and its DOS. Bond lengths are in Å and angles in degree.

3.2. AEM doping

A Zn atom in the tube wall has been substituted by four AEM atoms including Be, Mg, Ca, and Sr. E_{dop}, E_g, and Mulliken charge on dopant atoms are summarized in Table 1. The results indicate that the doping of AEM atoms on the Zn site is energetically favorable. The E_{dop} of Be (−4.62 eV) is much more negative than that of Mg (−2.40 eV), Ca (−1.26 eV), and Sr (−0.68 eV). This observation may be explained based on the Pearson's hard-soft acid–base theory (HSAB), which states that soft acids react strongly with soft bases, on the contrary, hard acids react strongly with hard bases, when all other factors being equal. The Be atom is a hard acid with smaller size compared to the Mg atom. Therefore, it tends to interact more preferably with oxygen atom which is known as a hard acid.

From the optimized structure (Fig. 2), it can be seen that all of the AEMs can significantly deform the ZnONT in the doped area except Mg. Be atom moves inward while Ca and Sr move outward from the tube wall due to their smaller and larger atomic radii than that of the zinc atom, respectively. Atomic radius of Mg is almost equal to that of zinc and it cannot deform the tube surface. Calculated lengths of Be–O bonds are about 1.526 and 1.558 Å in the Be@ZnONT, being much smaller than those of the corresponding Zn–O bonds in the pristine tube. Meanwhile, the Sr-doping leads to the largest structural deformation so that the Sr–O bonds are 2.459 and 2.517 Å (which significantly larger than Zn–O bond) and also corresponding angles are 95° and 100°.

Next, we have studied the influence of the AEM doping on the electronic properties of the ZnONT. Calculated DOS plots in Fig. 3 and data of Table 1 show that neither valence nor conduction levels of the tube are significantly changed after AEM doping, so the large E_g of ZnONT is completely preserved. For instance, in the case of Sr@ZnONT, E_g of the tube slightly decreases to 3.64 eV (3.7% change). Therefore, we believe that doping of the ZnONT with AEM may not significantly influence its electronic properties.

3.3. AM doping

The geometry structures were fully optimized to reach a stable structure for each AM doped ZnONT system. In contrast to AEM doping, it was found that AM doping is an energetically endothermic process ascribed to the smaller charge density on the AM ions in comparison with AEM ions. The E_{dop} becomes more positive and therefore energetically unfavorable in the order of Li < Na < K < Rb (Table 2). As can be seen in Fig. 4, a locally structural deformation at the doping site can be observed in all structures. In the case of

Table 1
Doping energy of AEM on ZnONT (E_{dop}), Mulliken charge on the doped adatom (Q_T), the HOMO, LUMO and gap (E_g) in between energies and Fermi level energy (E_{FL}) for different AEM-doped ZnONT systems. Energies are in eV.

System	E_{dop}	[a]QT (e)	E_{HOMO}	E_{FL}	E_{LUMO}	E_g	[c]ΔE_g (%)
ZnONT	–	[b]1.077	−6.32	−4.43	−2.55	3.77	–
Be−ZnONT	−4.62	0.874	−6.32	−4.42	−2.53	3.79	0.5
Mg−ZnONT	−2.4	1.474	−6.3	−4.41	−2.52	3.78	0.3
Ca−ZnONT	−1.26	1.492	−6.22	−4.35	−2.49	3.73	1.0
Sr−ZnONT	−0.68	1.625	−6.16	−4.34	−2.52	3.64	3.4

[a] QT is defined as the Mulliken charge on the AEM atom.
[b] The average Mulliken charge on the Zn atom.
[c] Change of Eg of ZnONT upon adsorption of metal atom.

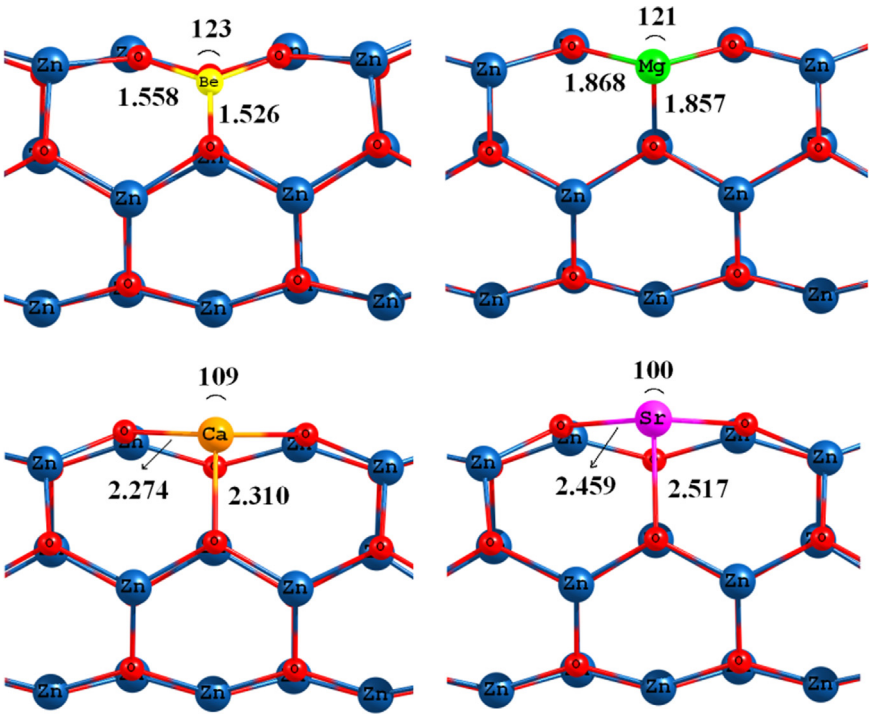

Fig. 2. Optimized structure of each AEM atom doped on ZnONT. Bond lengths in Å and angles in degree.

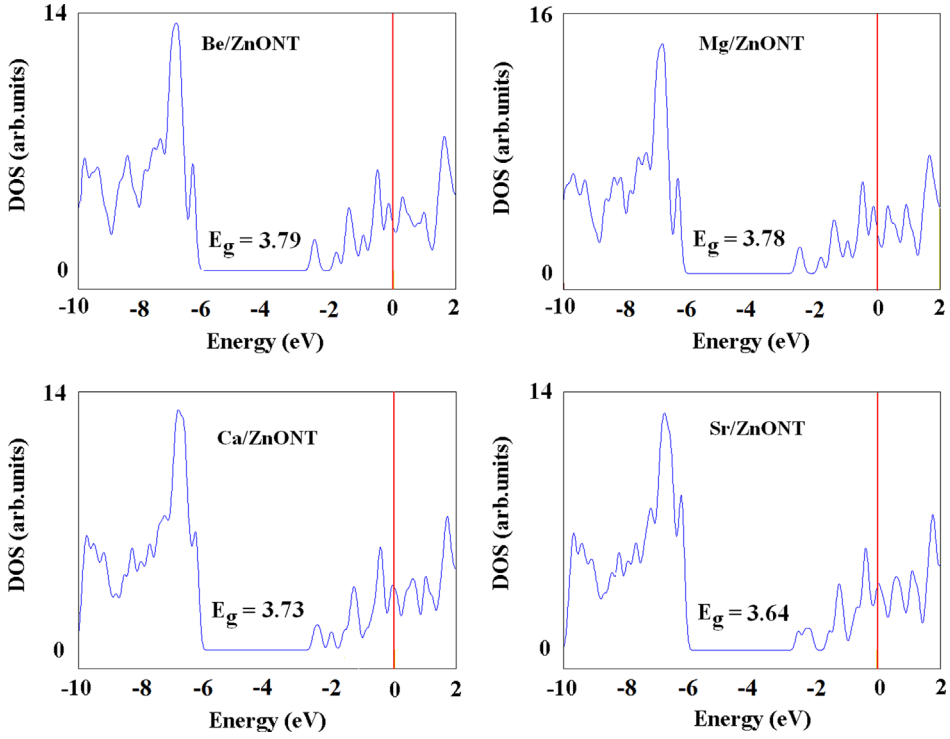

Fig. 3. Comparison between the DOS for different AEM-doped ZnONT.

Rb@ZnONT (Fig. 4d), the Rb atom and the three nearest neighbors of oxygen atoms move outward of the tube surface. This created lump is due to the larger radius of Rb compared to Zn. The bond lengths between doped Rb and three neighboring oxygen atoms are in the range of 2.796 – 2.883 Å. Interestingly, in the Li-doped case, hexagonal shape of the rings near the Li atom was destroyed and a four-square ring is formed (Fig. 4a). In this configuration, the O–Li–O angle is about 128° and the average bond lengths of newly formed Li–O and Zn–O are about 1.805 and 1.832 Å, respectively.

Furthermore, the transfer of charge between doped AM atom and ZnONT is estimated based on the popular Mulliken charge analysis, summarized in Table 2. We have found that some charges are transferred from AM atoms to the oxygen ones. The transferred charges of Li atom are significantly lower than that of Na, K, and Rb, which may be due to the smaller electron donating ability of Li than that of the other three atoms. Therefore, the AM can donate electrons more easily to its three bonded oxygen atoms than zinc atom in the pristine ZnONT, except in the case of Li.

Table 2
Doping energy of AM on ZnONT (E_{dop}, eV), Mulliken charge on the doped adatom (Q_T), the HOMO, LUMO and gap (E_g) in between energies (eV) and Fermi level energy (E_{FL}, eV) for different AM-doped ZnONT systems.

System	E_{dop}	[a]QT (e)	E_{HOMO}	E_{FL}	E_{LUMO}	E_g	[b]ΔE_g (%)
ZnONT	–	[b]1.077	−6.32	−4.43	−2.55	3.77	–
Li−ZnONT	0.78	0.439	−6.27	−5.29	−4.32	1.95	48.2
Na−ZnONT	1.03	0.897	−6.23	−5.39	−4.55	1.68	55.4
K−ZnONT	1.34	0.939	−6.16	−5.48	−4.81	1.35	64.2
Rb−ZnONT	1.86	1.004	−6.09	−5.53	−4.98	1.11	70.5

[a] Q_T is defined as the Mulliken charge on the AM atom.
[b] Change of E_g of ZnONT upon adsorption of metal atom.

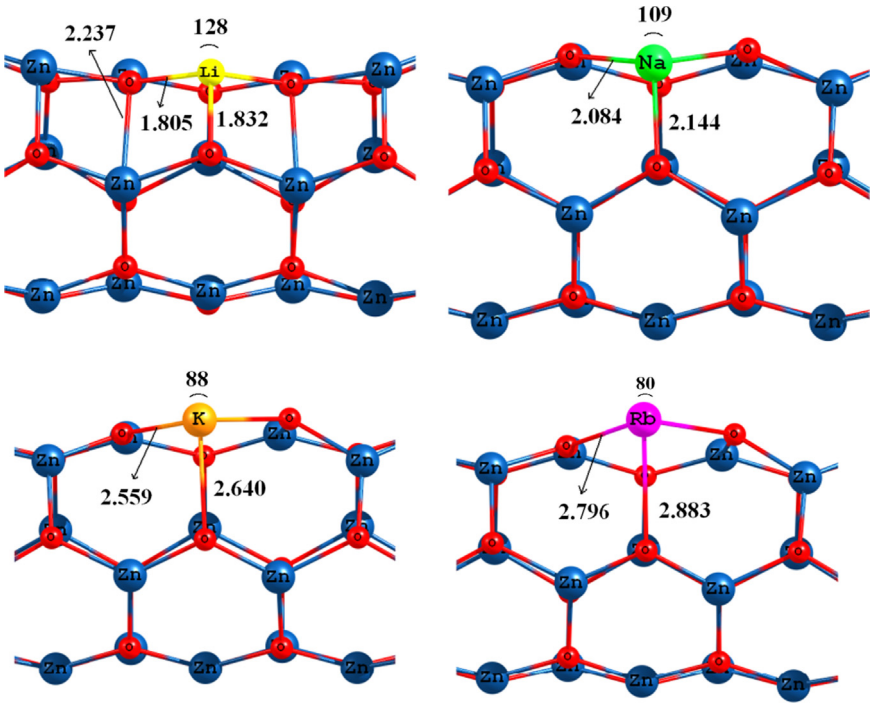

Fig. 4. Optimized structure of each AM atom doped into ZnONT. Bond lengths are in Å and angles in degree.

In order to consider the influence of doping on the electronic properties of the tube, the DOS plots for AM@ZnONT have been calculated. Since a small change of E_g can modify the electrical conductivity of the ZnONT, these changes (ΔE_g) upon the doping process are related to the sensitivity of the tube to a particular dopant. As shown by panels a–d in Fig. 5, the DOSs of the AM doped configurations have a distinct change near the conduction level compared to that of the pristine tube, so a local energy level appears after the adsorption of the metals. Therefore, upon the doping of AM, E_g of the tube is decreased from 3.77 eV in the bare ZnONT to 1.95 − 1.11 eV in doped forms. The largest decrement of E_g belongs to the case of Rb doping in which the E_g reduces from 3.77 to 1.11 eV (with 70.5% change) which would result in an electrical conductivity change of the nanotube according to the following equation:

$$\sigma \propto \exp\left(\frac{-E_g}{2kT}\right) \quad (2)$$

where σ is the electric conductivity, and k is the Boltzmann's constant [37]. According to the equation, smaller values of E_g at a given temperature lead to larger electric conductivity. However, smaller E_g of the complexes confirms its relative instability in comparison with the parent nanotubes.

Recently, there is great interest in field emission properties of ZnO nanostructures [38]. Based on FMO analysis, Fermi level of the ZnONT (−4.43 eV) slightly shifts to lower energies after AM doping (Table 2), whereas it shifts to higher energies upon the doping of AEM (Table 1). The canonical assumption for Fermi level is that in a molecule (at $T=0$ K) it lies approximately in the middle of the E_g. It is noteworthy to mention that, in fact, what lies in the middle of the E_g is the chemical potential, and since the chemical potential of a free gas of electrons, as traditionally defined, is equal to its Fermi level, herein, the Fermi level of the considered systems is at the center of the E_g. The change of Fermi level of a semiconductor upon the adatom doping alters its field emission currents. Since ZnO nanostructures are one of the promising candidates for field emitters, the present results are of great importance. It seems that the Ca-doped ($E_{FL}=-4.35$ eV) and Sr-doped ($E_{FL}=-4.34$ eV) will slightly facilitate the electron emission from the ZnONT surface. However, as shown in Table 2, the AM doping decreases the energy level of LUMO which can decrease Fermi level energy ($E_{FL}=-5.29$ to -5.53 eV). This phenomenon leads to an increment in the work function that is important in field emission applications. The work function can be found using the standard procedure by calculating the potential energy difference between the vacuum level and the Fermi level

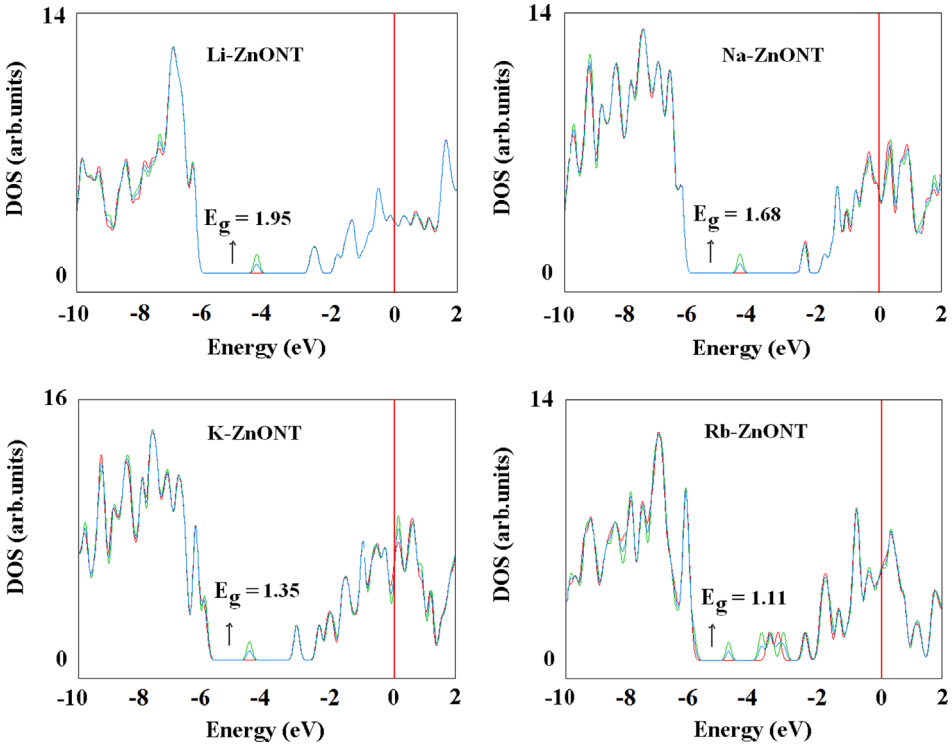

Fig. 5. Comparison among the density of states (DOS) of different AM-doped ZnONT.

Table 3
Energies of HOMO, LUMO, HOMO – LUMO gap (E_g) and Fermi level energy (E_{FL}) for different AEM – doped ZnONT systems. Energies are in eV.

System	E_{HOMO}	E_{FL}	E_{LUMO}	E_g	[a]ΔE_g (%)
ZnONT	−6.17	−4.42	−2.67	3.5	–
Be – ZnONT	−6.37	−4.5	−2.64	3.73	6.5
Mg – ZnONT	−6.21	−4.39	−2.57	3.64	4
Ca – ZnONT	−6.33	−4.47	−2.61	3.72	6.3
Sr – ZnONT	−6.07	−4.27	−2.48	3.59	2.5

[a] Change of E_g of ZnONT upon adsorption of metal atom.

Table 4
The HOMO, LUMO and gap (E_g) in between energies (eV) and Fermi level energy (EFL, eV) for different AM-doped ZnONT systems.

System	E_{HOMO}	E_{FL}	E_{LUMO}	E_g	[a]ΔE_g (%)
ZnONT	−6.17	−4.42	−2.67	3.5	–
Li–ZnONT	−6.2	−5.26	−4.33	1.87	46.5
Na–ZnONT	−6.26	−5.45	−4.64	1.62	53.7
K–ZnONT	−6.18	−5.51	−4.85	1.33	62
Rb–ZnONT	−6.01	−5.56	−5.11	0.9	74.3

[a] Change of E_g of ZnONT upon adsorption of metal atom.

which is the minimum energy required for one electron to be removed from the Fermi level to the vacuum. The increment in the work function indicates that the field electron emission current from the tube surface is impeded upon the adsorption of AM adatoms. The HSE (Heyd-Scuseria-Ernzerhof) [39] exchange-correlation functional with LANL2DZ basis set was also used to calculate the electronic properties of the studied systems. The results in Tables 3 and 4 show that although the values of E_g is somewhat smaller than those of the B3LYP, contrary to the AEM doping, the electronic properties of the tube are much more sensitive to AM doping. Like the B3LYP, the HSE functional indicates that the doping of alkali and alkaline metals increases and decreases the work function of the tube, respectively.

4. Conclusion

We have studied the doping of different AM and AEM atoms into the sidewall of an armchair ZnONT using density functional calculations. We have found that doping processes of AEM are exothermic and E_{dop} is in the range of −4.62 to −0.68 eV, while those of AM are endothermic. Also, contrary to the AEM doping, the electronic properties of the tube are much more sensitive to AM doping. The AM doping and AME doping increases and decreases the work function of the tube, respectively, influencing the electron emission current from the tube surface.

References

[1] S. Iijima, Nature 354 (1991) 56.
[2] G. Yu, G. Tang, Y. Jia, L. Wu, Physics Letters A 376 (2012) 1948.
[3] X.X. Wang, X.Y. Li, H.N. Li, Physics Letters A 372 (2008) 6677.
[4] K. Tsukagoshi, N. Yoneya, S. Uryu, Y. Aoyagi, A. Kanda, Y. Ootuka, B.W. Alphenaar, Physica B 323 (2002) 107.
[5] B. Bellafi, S. Haddad, I. Sfar, S. Charfi-Kaddour, Physica B 404 (2009) 524.
[6] A. Ahmadi, N.L. Hadipour, M. Kamfiroozi, Z. Bagheri, Sensors and Actuators B 161 (2012) 1025.
[7] J. Beheshtian, M.T. Baei, A.A. Peyghan, Surface Science 606 (2012) 981.
[8] Y. Zhang, Y.H. Wen, J.C. Zheng, Z.Z. Zhu, Physics Letters A 374 (2010) 2864.
[9] A. Ahmadi, J. Beheshtian, N.L. Hadipour, Physica E 43 (2011) 1717.
[10] J. Beheshtian, M. Kamfiroozi, Z. Bagheri, A. Ahmadi, Physica E 44 (2011) 546.
[11] J. Beheshtian, H. Soleymanabadi, M. Kamfiroozi, A. Ahmadi, Journal of Molecular Modeling 18 (2012) 2343.
[12] J. Beheshtian, M.T. Baei, Z. Bagheri, A.A. Peyghan, Microelectronics Journal 43 (2012) 452.
[13] M. Caglar, S. Ilican, Y. Caglar, F. Yakuphonoglu, Materials Chemistry and Physics 114 (2009) 194.
[14] T. Sahoo, S.K. Tripathy, Y.T. Yu, H.K. Ahn, D.C. Shin, I.H. Lee, Materials Research Bulletin 43 (2008) 2060.
[15] M. Willander, Q.X. Zhao, Q.H. Hu, P. Klason, V. Kuzmin, S.M. Al-Hilli, O. Nur, Y.E. Lozovik, Superlattices and Microstructures 43 (2008) 352.

[16] R.Y. Hong, J.H. Li, L.L. Chen, D.Q. Liu, H.Z. Li, Y. Zheng, J. Ding, Powder Technology 189 (2009) 426.
[17] J. Beheshtian, A.A. Peyghan, Z. Bagheri, Applied Surface Science 258 (2012) 8171.
[18] H. Xu, R.Q. Zhang, X. Zhang, A.L. Rosa, T. Frauenheim, Nanotechnology (2007) 485713(1).
[19] D.P. Yu, Nanowires and Nanobelts: Metals and Semi- conductor Nanowires, in: Z.L. Wang (Ed.), Kluwer Academic, New York, 2003.
[20] M.M. Husain, Physica E 41 (2009) 1329.
[21] S. Erkoc, H. Kokten, Physica E 28 (2005) 162.
[22] H. Xu, F. Zhan, A.L. Rosa, Th. Frauenheim, R.Q. Zhang, Solid State Communications 148 (2008) 534.
[23] F. Gao, J. Hu, J. Wang, C. Yang, H. Qin, Chemical Physics Letters 488 (2010) 57.
[24] F.C. Zhang, Z.Y. Zhang, W.H. Zhang, J.F. Yan, J.N. Yun, Chinese Physics Letters 26 (2009) 016105(1).
[25] J.H. He, C.S. Lao, L.J. Chen, D.G. Davidovic, Z.L. Wang, Journal of the American Chemical Society 127 (2005) 16376.
[26] K.R. Kittilstved, D.R. Agmelin, Journal of the American Chemical Society 127 (2005) 5292.
[27] G. Chai, C. Lin, J. Wang, M. Zhang, J. Wei, W. Cheng, Physical Chemistry C 115 (2011) 2907.
[28] C. Hui Zhang, Q. Ran, J. Shen, Advanced Materials Research 320 (2011) 410–414.
[29] M. Schmidt, et al., Journal of Computational Chemistry 14 (1993) 1347.
[30] N. O'Boyle, A. Tenderholt, K. Langner, Journal of Computational Chemistry 29 (2008) 839.
[31] T.C. Dinadayalane, J.S. Murray, M.C. Concha, P. Politzer, J. Leszczynski, Journal of Theoretical and Computational Chemistry 6 (2010) 1351.
[32] J. Beheshtian, Z. Bagheri, M. Kamfiroozi, A. Ahmadi, Microelectronics Journal 42 (2011) 1400.
[33] M. Contreras, D. Avila, J. Alvarez, R. Rozas, Structural Chemistry 21 (2010) 573.
[34] M. Breza, Chemical Physics 330 (2006) 224.
[35] J. Sun, H.T. Wang, J.L. He, Y.J. Tian, Physical Review B 71 (2005) 125132(1).
[36] Y.L. Mao, X.H. Yan, Y. Xiao, J. Xiang, Y.R. Yang, H.L. Yu, Nanotechnology 15 (2004) 1000.
[37] S. Li, Semiconductor Physical Electronics, Second ed., springer, USA, 2006.
[38] W. Lee, M.C. Jeong, M.J. Kim, J.M. Myoung, Physics Letters A 370 (2007) 345.
[39] J. Heyd, G.E. Scuseria, M. Ernzerhof, Journal of Chemical Physics 118 (2003) 8207.